23rd ABCM International Congress of Mechanical Engineering
December 6-11, 2015, Rio de Janeiro, RJ, Brazil

ANALYSIS OF ROTORS SUPPORTED BY THRUST BEARINGS

Thales Freitas Peixoto
Leonardo Carpinetti Vieira
Katia Lucchesi Cavalca
FEM/UNICAMP – Faculty of Mechanical Engineering – University of Campinas
Av. Mendeleyev, 200, 13083-970, Cidade Universitária Zeferino Vaz, Barão Geraldo – Campinas-SP, Brazil
thalesfp@fem.unicamp.br. leonardo.cv@uol.com.br, katia@fem.unicamp.br

Abstract: *The assembly of a rotary machine, with a rotating shaft supported by bearings, is called rotor. A very specific class of rotors is the high rotation turbocharger to automotive application. In these turbochargers, the shaft where the rotors are mounted is continually subjected to an axial force because of the gas acting on the turbine and of the air on the compressor with different magnitudes, causing an axial displacement of the shaft, which must be supported by the axial lubricated bearing. Therefore, thrust bearings are necessary to absorb these forces and displacements, avoiding direct contact between the solid surfaces, which means that the lubricated thrust bearings must be designed so that the fluid film sustain the shaft axially, avoiding friction and premature wear in the bearing surface. In this work, models of segmented thrust bearings of fixed geometry are used, which are linearly modeled by equivalent stiffness and damping dynamic coefficients. Numerical simulations are accomplished utilizing a model of concentrated parameters, in which the mass is concentrated in the shaft collar, and a model by finite element method (FEM), wherein the shaft, rotors and bearings are properly discretized. The sensitivity of the thrust bearing model to the discretization is analyzed and the response of the system to impulse and step inputs are obtained and compared for both models of the system. Significant parameters like natural frequencies and the displacement amplitudes at the collar node are also evaluated and compared.*

Keywords: *Hydrodynamic Thrust Bearings, Rotor Dynamic Analysis, Stiffness and Damping Coefficients.*

1. INTRODUCTION

A rotary machine is the assembly of a rotating shaft supported by bearings, with one or more rotors (turbine or compressor). A very specific class of rotors are turbocharges to automotive application. A turbocharger is an equipment added to the internal combustion engines to raise the power of the engine. The shaft is the element responsible to transfer the energy from the turbine to the compressor and the bearings are responsible to support the loadings on the shaft. Due to the gas flows in the turbine and the compressor are not constant, axial forces with different magnitudes are generated, inducing axial displacements in the shaft that must be supported by lubricated thrust bearings. Therefore, lubricated thrust bearings must be designed to support the shaft axially, preventing contact between the surfaces of the thrust bearing and the shaft collar to avoid friction and premature wear. The objective of this paper is to analyze the axial vibration in rotating systems, in particular the turbocharger, considering lubricated thrust bearings models. The shaft is modeled by lumped parameters and by finite element method. The finite elements are bar elements, because the focus is on the axial vibration of the shaft. The dynamic characteristics of the thrust bearings are approached by equivalent stiffness and damping coefficients, obtained by Vieira (2014). The sensitivity of the thrust bearing model to the discretization is analyzed and the response of the system to impulse and step inputs are obtained and compared for both models of the system. Significant parameters like natural frequencies and the displacement amplitudes at the collar node are also evaluated and compared.

2. METHODOLOGY

The system is modeled by lumped parameters model and finite element model. In the first model, the total mass of the system is concentrated in the collar attached to the shaft, while in the second model, the shaft is discretized by finite elements.

Finally, an analytical model is also applied and compared to both discrete models to verify the evaluation of natural frequencies and the convergence of the discrete models.

2.1. Equations of Motion

The equations of motion of the vibratory system can be described by a system of differential equations subjected to initial conditions:

$$[M_G]\{\ddot{u}\} + [C_G]\{\dot{u}\} + [K_G]\{u\} = \{F(t)\}, \quad \{u(t_0)\} = \{u_0\}, \{\dot{u}(t_0)\} = \{\dot{u}_0\} \tag{1}$$

where $[M]$ is the mass matrix (inertia matrix), $[C]$ is the damping matrix and $[K]$ is the stiffness matrix and the subscript G stands for *global* (i.e. the global mass matrix, the global damping matrix and the global stiffness matrix). The vectors $\{u\}$, $\{\dot{u}\}$ and $\{\ddot{u}\}$ contain the displacement, the velocity and the acceleration of each degree of freedom of the structure and $\{F\}$ is the vector of external excitation forces. The mass, damping and stiffness matrix can be obtained by the finite element method. In the finite element method, the shaft is modeled by bar elements able to vibrate axially. Hence, shape functions are used to interpolate the solution between the discrete values obtained at the nodes of the structure. For a unidimensional linear bar element, the shape functions are $[N] = \begin{bmatrix} \frac{L-x}{L} & \frac{x}{L} \end{bmatrix}$. The global mass and stiffness matrices are obtained assembling the elementary matrices (Cook, et al., 2002):

$$[M_E] = \int_0^L \rho [N]^T [N] dx = \frac{\rho A L}{6} \begin{bmatrix} 2 & 1 \\ 1 & 2 \end{bmatrix}, \quad [K_E] = \int_0^L [B]^T E [B] A dx = \frac{EA}{L} \begin{bmatrix} 1 & -1 \\ -1 & 1 \end{bmatrix} \tag{2}$$

where ρ is the density of material, A, the cross-sectional area of the bar, L, its length, E, its elasticity modulus and $[B]$ is the derivative vector of the shape functions ($[B] = d[N]/dx$). The global damping matrix is considered structural proportional as a linear combination of the mass and stiffness matrices ($[C_G] = \mu[M_G] + \lambda[K_G]$), as firstly introduced by Rayleigh (1877) in the concept of modal analysis, whose coefficients μ and λ must be carefully chosen.

To account for the other elements of the structure, models of rigid discs are used to the collar connected to the shaft, and stiffness and damping equivalent coefficients to the thrust bearing, analogously to the finite element model of the rotor introduced by Nelson & McVaugh (1976) and Nelson (1980). The rigid discs contribution to the model is mainly in terms of mass and inertia, so these elements have only a mass matrix $[M_D]$ which places the mass of each disc on its correspondent degree of freedom. The thrust bearings coefficients are obtained solving the Reynolds equation and the energy equation simultaneously, in order to obtain the pressure and the temperature distribution of the oil film between the bearing pads and the shaft collar (Vieira & Cavalca, 2009). These coefficients are placed on the correspondent degree of freedom of the thrust bearing at the shaft in the stiffness and damping matrices.

If the mass of the entire system is concentrated in the collar, as illustrated by Fig.1 then a simpler model is obtained, the lumped parameters model. In this model, only the position of the collar is observed and the governing equation of motion is the single degree of freedom equation, namely, the mass-spring-damper system, which can be rewritten using the modal parameters ($\omega_n = \sqrt{K_{xx}/M}$, $\xi = C_{xx}/\sqrt{K_{xx}M}$) and observing that $f(t) = F(t)/M$:

$$M\ddot{x} + C_{xx}\dot{x} + K_{xx}x = F(t) \rightarrow \ddot{x} + 2\xi\omega_n\dot{x} + \omega_n^2 x = f(t) \tag{2}$$

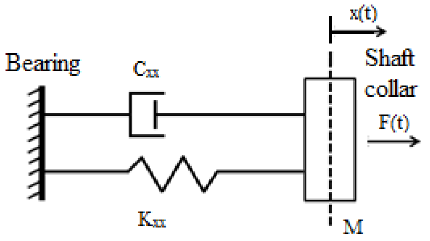

Figure 1. Mass-spring-damper lumped system (adapted from Vieira, 2014)

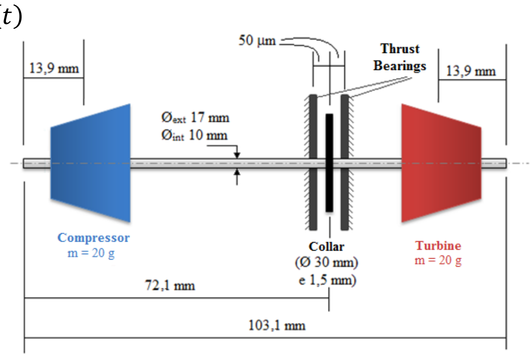

Figure 2. Scheme of the Turbocharger system.

2.2. Fundamental Matrix and General Solution

The solution of the system described by Eq. (1) to an external excitation can be obtained from the state equation (Müller & Schiehlen, 1985). The state equation is defined as:

$$\{\dot{y}(t)\} = [A]\{y(t)\} + \{B(t)\}, \{y(t_0)\} = \{y_0\} = \begin{Bmatrix} \{u_0\} \\ \{\dot{u}_0\} \end{Bmatrix} \tag{3}$$

where $\{y(t)\}$ is the state vector, formed from both the position and velocity vectors.

The matrix $[A]$ in Eq. (3) is called the state space matrix, and is given as:

$$[A] = \begin{bmatrix} [0] & [I] \\ -[M_G]^{-1}[K_G] & -[M_G]^{-1}[C_G] \end{bmatrix} \tag{4}$$

where $[0]$ is a $n \times n$ zero matrix and $[I]$ is the $n \times n$ identity matrix (n is the number of the degrees of freedom and, therefore, the size of the square matrices $[M_G]$, $[C_G]$ and $[K_G]$). $\{B(t)\}$ is called the excitation vector:

$$\{B(t)\} = \begin{Bmatrix} \{0\} \\ [M_G]^{-1}\{F(t)\} \end{Bmatrix} \tag{5}$$

The homogeneous linear system of differential equations of order $2n$ allows the analysis of the eigenproblem, to obtain the modal parameters of the system (Gupta, 1974), and always has a fundamental system of $2n$ linearly independent solution vectors $\{\varphi_i(t)\}$, $i = 1(1)2n$, which coincide for $t = 0$ with the $2n$ unit vectors $\hat{e}_i$,

$$\{\varphi_i(0)\} = \hat{e}_i, i = 1(1)2n \tag{6}$$

and satisfy the homogeneous equation:

$$\{\dot{\varphi}_i(t)\} = [A]\{\varphi_i(t)\} \tag{7}$$

These solution vectors form the columns of a regular $2n \times 2n$ matrix, called the fundamental matrix:

$$[\Phi(t)] = [\{\varphi_1(t)\} \quad \{\varphi_2(t)\} \quad \cdots \quad \{\varphi_n(t)\}] \tag{8}$$

The general solution of Eq. (3) is the general solution of the homogeneous system $\{y_h(t)\}$ added to a particular solution $\{y_p(t)\}$ of Eq. (3). The solution to the homogenous system with initial conditions $\{y_0(t)\} = \{y_0\}$ is obtained as a linear combination of the fundamental solutions (Müller & Schiehlen, 1985):

$$\{\dot{y}(t)\} = \sum_{i=1}^{n} \{\varphi_i(t)\} y_{i0} = [\Phi(t)]\{y_0\} \tag{9}$$

which can be rewritten using the fundamental matrix.

The particular solution can be found by the method of variation of constants (Müller & Schiehlen, 1985):

$$\{y_p(t)\} = \int_0^t [\Phi(t-\tau)]\{B(\tau)\} d\tau \tag{10}$$

2.3. Impulse Response

Impulsive excitation forces can be represented by the Dirac function $\delta(t - t_I)$

$$\{B(t)\} = \{B_I\}\delta(t - t_I) \tag{11}$$

where $\{B_I\}$ is a constant vector and t_I is the instant of the impulse. The state equation of a system excited by an impulse is:

$$\{\dot{y}(t)\} = [A]\{y(t)\} + \{B_I\}\delta(t - t_I), \{y(0)\} = \{y_0\} \tag{12}$$

And the correspondent impulsive solution is (Müller & Schiehlen, 1985):

$$\{y_I(t)\} = [\Phi(t)]\{y_0\} + \int_0^t [\Phi(t-\tau)]\{B_I\}\delta(t - t_I) d\tau = \begin{cases} [\Phi(t)]\{y_0\}, 0 \le t < t_I \\ [\Phi(t)](\{y_0\} + [\Phi(-t_I)]\{B_I\}), t > t_I \end{cases} \tag{13}$$

It can be observed that the impulsive excitation causes a step change of the state variables at the instant of the impulse, which means that, for the time instant immediately after the impulse:

$$\begin{Bmatrix} \{u_I\} \\ \{\dot{u}_I\} \end{Bmatrix} = [\Phi(t_I)] \begin{Bmatrix} \{u_0\} \\ \{\dot{u}_0\} \end{Bmatrix} + \begin{Bmatrix} \{0\} \\ [M_G]^{-1}\{B_I\} \end{Bmatrix} \tag{14}$$

2.4. Step Response

Step excitation forces can be represented by the step function $s(t - t_S)$:

$$\{B(t)\} = \{B_S\}s(t - t_S) \tag{15}$$

where $\{B_S\}$ is a constant vector and t_S is the instant of the step. The correspondent state equation of a system excited by a step is:

$$\{\dot{y}(t)\} = [A]\{y(t)\} + \{B_S\}s(t - t_I), \{y(0)\} = \{y_0\} \tag{16}$$

The step solution with $\{y_\infty\} = -[A]^{-1}\{B_S\}$ is (Müller & Schiehlen, 1985):

$$\{y_I(t)\} = [\Phi(t)]\{y_0\} + \int_0^t [\Phi(t-\tau)]\{B_S\}s(t - t_S)d\tau = \begin{cases}[\Phi(t)]\{y_0\}, 0 \le t < t_S \\ [\Phi(t)]\{y_0\} + ([I] - [\Phi(t - t_S)])\{y_\infty\}, t > t_S\end{cases} \tag{17}$$

It can be observed from Eq. (17) that the step excitation causes a change in the equilibrium position of the system, at the instant of the step, which means that the motion consists of natural vibration around the new equilibrium position.

2.5. Analytical Equation

The governing equation for longitudinal oscillation of a uniform bar of length L is (Balachandram & Magrab, 2009):

$$AE\frac{\partial^2 u}{\partial x^2} - A\rho\frac{\partial^2 u}{\partial t^2} = f(x,t) \tag{18}$$

where the parameters are the same as for the finite element discretization of the system, i.e., A is the cross-sectional area of the bar, E is the modulus of elasticity, ρ is the specific mass, $u = u(x,t)$ is the displacement of the bar, as a function of the spatial variable x and the temporal variable t, and f is the exciting function.

From Eq. (18), the analytical natural frequencies of an axially loaded system can be obtained. If the bar has a mass m attached to a position l_m, a viscous damper c attached to a position l_d or a spring k attached to a position l_k, $0 \le l_m, l_d, l_k \le L$, then these discontinuities can be represented in the equation using the Dirac function as $m\delta(x - l_m)\frac{\partial^2 u}{\partial t^2}$, $c\delta(x - l_d)\frac{\partial u}{\partial t}$, $k\delta(x - l_s)u$. To obtain the natural frequencies, no external forces are assumed and the bar is subjected to harmonic oscillation, $u(x,t) = U(x)e^{j\omega t}$. The Laplace transform technique is employed to obtain the frequency equation. To calculate the analytical natural frequencies of the system schematically represented in Fig. 2, the compressor and turbine are modeled as concentrated masses m_c and m_t, respectively at positions l_c and l_t. The thrust bearing is modeled as a collar of mass m_b, a spring stiffness k_b and a viscous damper c_b, at position l_b, representing the equivalent coefficients of the bearing. The analytical natural equation of this system is:

$$EA\frac{\partial^2 u}{\partial x^2} - \left(\rho A + m_c\delta(x - l_c) + m_b\delta(x - l_d) + m_t\delta(x - l_t)\right)\frac{\partial^2 u}{\partial t^2} - k_b\delta(x - l_b) - c_b\delta(x - l_b)\frac{\partial u}{\partial t} = 0 \tag{19}$$

with boundary conditions $\partial u(0,t)/\partial x = 0$ and $\partial u(L,t)/\partial x = 0$. It is important to notice that a viscous damper does not alter the natural frequencies of the system, so, to obtain the natural frequencies, it can be assumed $c_b = 0$ without loss of generality. Assuming harmonic motion, $u(x,t) = U(x)e^{j\omega t}$, substituting its derivatives in Eq. (19) and applying the Laplace transform gives:

$$EA\left(s^2\bar{U} - sU(0) - U'(0)\right) + \rho A\omega^2\bar{U} + m_c\omega^2 e^{-l_c s}U(l_c) + m_b\omega^2 e^{-l_b s}U(l_b) + m_t\omega^2 e^{-l_t s}U(l_t) - k_b e^{-l_b s}U(l_b) = 0 \tag{20}$$

where $\bar{U} = \bar{U}(s) = \mathcal{L}\{U(x)\}$. Rearranging and applying the inverse Laplace transform, with $c = \sqrt{\rho/E}$ gives:

$$U(x) = U(0)\cos(c\omega x) + \frac{U'(0)}{c\omega}\sin(c\omega x) - f_1(x,\omega) - f_2(x,\omega) - f_3(x,\omega) \tag{21}$$

where:

$$\begin{aligned} f_1(x,\omega) &= (m_c\omega/EAc)\sin\left(c\omega(x - l_c)\right)s(x - l_c) \\ f_2(x,\omega) &= (m_b\omega/EAc - k/EAc\omega)\sin\left(c\omega(x - l_b)\right)s(x - l_b) \\ f_3(x,\omega) &= (m_t\omega/EAc)\sin\left(c\omega(x - l_t)\right)s(x - l_t) \end{aligned} \tag{22}$$

Applying the boundary condition $U'(0) = 0$,

$$U(x) = U(0)\cos(c\omega x) - f_1(x,\omega)U(l_c) - f_2(x,\omega)U(l_b) - f_3(x,\omega)U(l_t) \tag{23}$$

It is necessary to obtain $U(0)$ and the other boundary condition $U'(L) = 0$ can be used. Deriving Eq. (23) and substituting $U'(L) = 0$,

$$U'(L) = -c\omega U(0)\sin c\omega L - f_1'(L,\omega)U(l_c) - f_2'(L\omega)U(l_b) - f_3'(L,\omega)U(l_t) = 0 \tag{24}$$

Equation (24) can be rearranged to obtain $U(0)$. Substituting $U(0)$ in Eq. (23):

$$U(x) = g_1(x,\omega)U(l_c) + g_2(x,\omega)U(l_b) + g_3(x,\omega)U(l_d) \tag{25}$$

where

$$\begin{aligned} g_1(x,\omega) &= -\frac{m_c\omega}{EAc}\frac{\cos\big(c\omega(L-l_c)\big)}{\sin(c\omega L)} - f_1(x,\omega) \\ g_2(x,\omega) &= -\frac{1}{EAc}\left(m_b\omega - \frac{k}{\omega}\right)\frac{\cos\big(c\omega(L-l_b)\big)}{\sin(c\omega L)} - f_2(x,\omega) \\ g_3(x,\omega) &= -\frac{m_t\omega}{EAc}\frac{\cos\big(c\omega(L-l_t)\big)}{\sin(c\omega L)} - f_3(x,\omega) \end{aligned} \tag{26}$$

Equation (25) must be satisfied at the discontinuities l_c, l_b and l_t, which gives the system of equations (27). Imposing the determinant of the coefficients matrix in Eq. (27) to be zero leads to the frequency dependent equation, which can be numerically evaluated.

$$\begin{bmatrix} 1-g_1(l_c,\omega) & -g_2(l_c,\omega) & -g_3(l_c,\omega) \\ -g_1(l_b,\omega) & 1-g_2(l_b\omega) & -g_3(l_b,\omega) \\ -g_1(l_t,\omega) & -g_2(l_t,\omega) & 1-g_3(l_t,\omega) \end{bmatrix} \begin{Bmatrix} U(l_c) \\ U(l_d) \\ U(l_t) \end{Bmatrix} = \begin{Bmatrix} 0 \\ 0 \\ 0 \end{Bmatrix} \tag{27}$$

3. RESULTS AND GENERAL COMMENTS

The simulated system is illustrated in Fig. 2. This system is a simplified model of a turbocharger, considering the shaft and the collar, the thrust bearings (responsible for the damping of the system), and the turbine and compressor, both modeled as lumped masses. The total mass of the system is 165 g. The clearance between the collar and the thrust bearing is the physical thickness where the oil film circulates. The equivalent coefficients of the bearing are estimated by Vieira (2014) for two different rotation speeds. These values are shown in Tab. 1.

Table 1. Equivalent stiffness and damping coefficients of the thrust bearing for two rotation speed (Vieira, 2014)

N (rpm)	K_{xx} (10^6 N/m)	C_{xx} (10^3 N.s/m)
14100	4.572	4.264
20280	7.030	4.339

With these values, it is possible to simulate the impulse response and the step response of the system. The impulse response is obtained with the objective of observing certain characteristics of the system, when excited with a unit impulse. The step response is obtained because Zhu & Zhang (2003) propose to simulate the force of the turbine as a step with arbitrary amplitude $F(t) = \Delta F s(t)$. The influence of both the shaft and the bearing discretization are observed in the system response. The relevant parameter is the displacement of the collar in time. In the simulations, the shaft is made of steel ($E = 210\ GPa$, $\rho = 7800\ kg/m^3$), with a cross-sectional area of $A = 1.484 \cdot 10^{-4}\ m^2$.

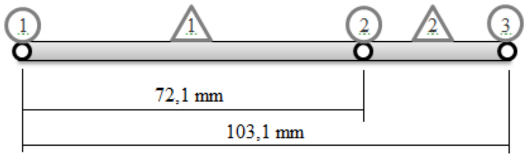

Figure 3. Mesh 1: Coarse mesh of the shaft (2 elements)

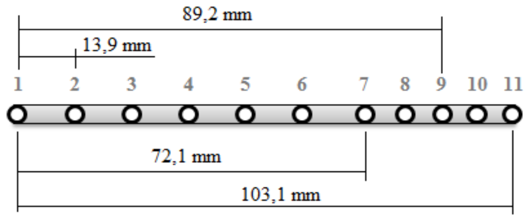

Figure 4. Mesh 2: Shaft discretization (10 elements)

The response is also compared to the lumped parameters model. The dynamic responses of the systems discretized by finite elements are calculated using the Newmark integration method (Newmark, 1959), with $\alpha = 0.5$ and $\delta = 0.25$. With these values, the integration method is unconditionally stable (Bathe & Wilson, 1973), which means that the integration process converges for any time step.

3.1. Mesh 1: coarse mesh of the shaft

The first finite element mesh is showed in Fig. 3. In this mesh, the shaft is divided in two elements.

The compressor is located on node 1 and the turbine, on node 3. The collar and the bearing are located on node 2. This system is simulated to an impulse and to a step external excitation force applied at the turbine (node 3).

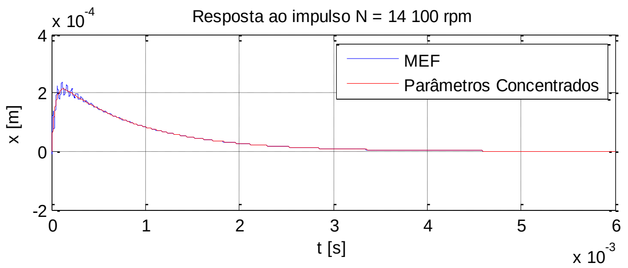

Figure 5. Unit impulse response at the collar (node 2), 14100 rpm

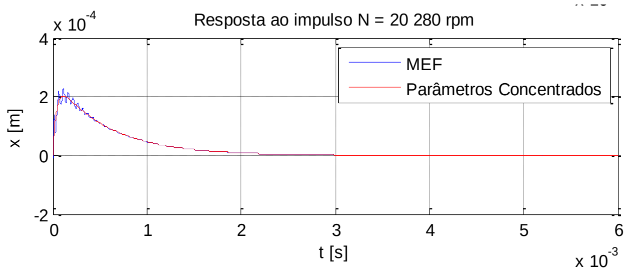

Figure 6 – Unit impulse response at the collar (node 2), 20280 rpm

Figures 5 and 6 show the response for the unit impulse excitation, and Figs. 7 and 8, for the unit step excitation, for both rotational speeds. The unit impulse response is in agreement for the finite element model and the lumped parameter (the tendency of the curve is the same in both cases). However, the finite element model presents a vibration of high frequency component due to the three vibration modes associated to the three degrees of freedom of the first mesh (3 nodes). The first mode corresponds to the first natural frequency, the same found to the lumped parameters model. The other high frequencies modes are responsible for the oscillation around the first mode response. It is also observed that the system is stable and rapidly tends to the equilibrium position. In the unit step response, the influence of high frequencies modes can be neglected.

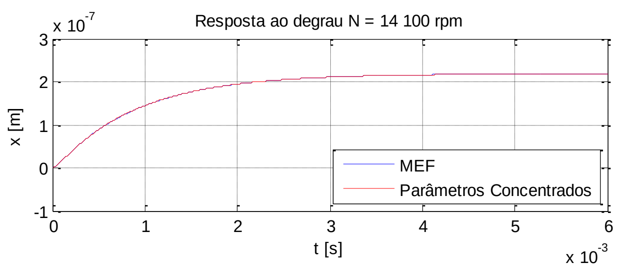

Figure 7. Unit step response at the collar (node 2), 14100 rpm

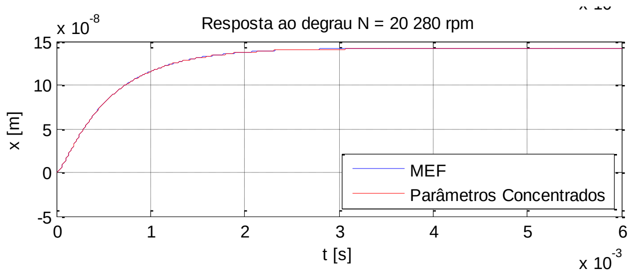

Figure 8. Unit step response at the collar (node 2), 20280 rpm

3.2. Mesh 2: Shaft discretization

The influence of the shaft discretization in the system response is analyzed here. The mesh is represented in Fig. 4. In this case, the compressor is located on node 2 and the turbine on node 9. The bearing and the collar are both located at node 7. This system is excited with a unit impulse and the time response is observed in Figs. 9 and 10. The shaft discretization does not significantly affect the response at the collar position (node 7), but it permits to observe the shaft deformation, along with the collar displacement. The vibration of high frequency is still observed when compared to the lumped parameters model, at the same frequency observed in Fig. 5 and 6 reported in Tab. 2.

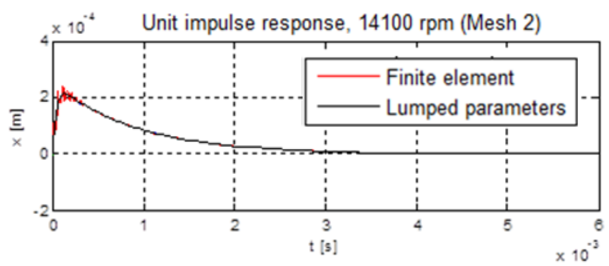

Figure 9. Impulse response (10 elements), 14100 rpm

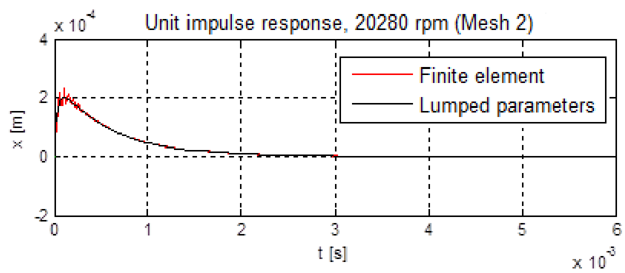

Figure 10. Impulse response (10 elements), 20280 rpm

3.3. Mesh 3: Bearing discretization

It is also possible to discretize the bearing in five nodes, considering one node on each thrust bearing, one node on the collar and one node in each film thickness between the bearings and the collar (Fig.11). In this finite element model, the collar is on node 4, where the disc mass is also located, and the equivalent coefficients of the bearing are added to nodes 3 and 5. The equivalent coefficients, in this case, are half of the coefficients presented in Tab. 1 (it is assumed each bearing is responsible for half of the stiffness and damping of the structure). The inertias of both compressor and turbine are located on nodes 1 and 7, respectively.

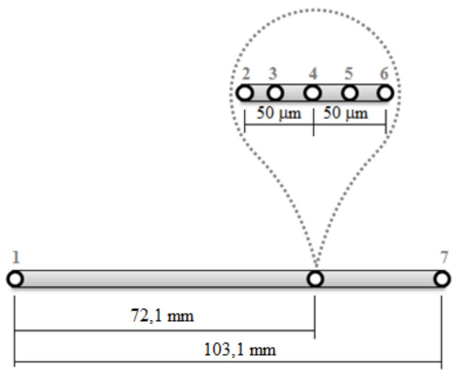

Figure 11. Mesh 3: Bearing discretization (6 elements)

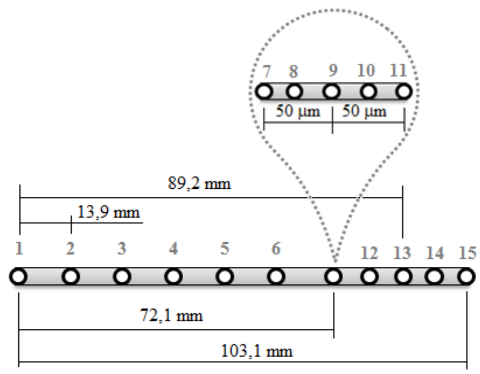

Figure 12. Mesh 4: Shaft and bearing discretization (14 elements)

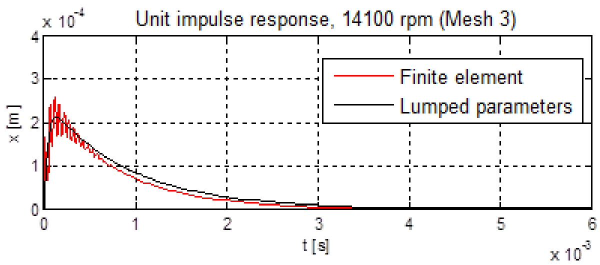

Figure 13. Impulse response (6 elements), 14100 rpm

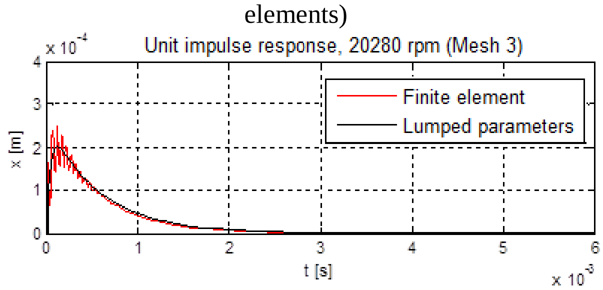

Figure 14. Impulse response (6 elements), 20280 rpm

The unit impulse response of the collar (node 4) is presented in Figs. 13 and 14. This model requires more computational time, since the matrices can be eventually ill-conditioned due to the very small length of the elements into the bearing discretization. Also, it is observed that the vibration amplitude of the high frequency modes is higher than in the previous cases due to the bearings degrees of freedom. However, this mesh has some advantages, for instance, to take into account different bearings, with different equivalent coefficients. Hence, this finite element model allows to observe the influence of each bearing individually in the system.

3.4. Mesh 4: Shaft and Bearing discretization

The last discretization concerns to the response to a unit impulse of the system when both the shaft and the bearing are discretized. The mesh is represented in Fig. 12 and the unit impulse response of the collar is presented in Figs. 15 and 16.

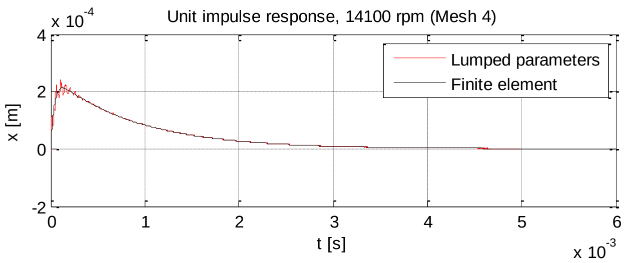

Figure 15. Impulse response (14 elements), 14100 rpm

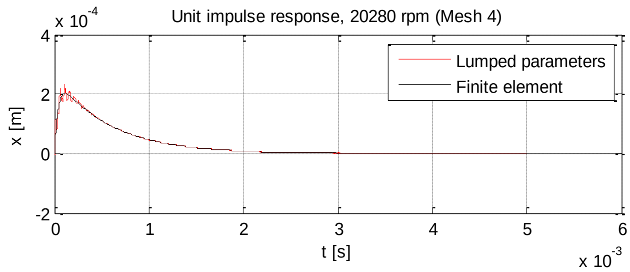

Figure 16. Impulse response (14 elements), 20280 rpm

It can be observed that the high frequency vibration is still present, similarly to the response in Figs. 13 and 14 (mesh 3) due to the bearing discretization. However, the predominant mode is again in agreement with the response of the lumped parameters model. This model has all the advantages discussed in Sections 3.2 and 3.3, along with the problems of the bearing discretization – possibility of ill-conditioned matrices, which increases the computational time of the simulation. However, not only it is possible to observe the displacement of the bearing, along with (possibly) using two different equivalent coefficients for each thrust bearing, it also allows the analysis of the deformation along the shaft.

3.5. Natural frequencies of the system

The discretization of the shaft introduces high-frequency modes, not observed when the lumped model is considered. To check if these modes are, in fact, presented in the structure, the natural frequencies of the finite element meshes were evaluated, along with the natural frequencies of the analytical solution presented in section 2.5. The system in Fig. 2 is considered with the compressor and turbine modeled as concentrated masses of 20 grams each, at positions 13.9 mm and 89.2 mm, respectively. The bearings are modeled with the rigid disc, at position 72.1 mm, with a spring and a viscous damper presented in Tab. 1. The analytical natural frequencies are obtained and presented in Tab. 2, which also presents the results from the state space matrix in the finite element model and the natural frequency given by the lumped parameters model. Table 2 shows that the first natural frequency estimated by the finite element method has an error of 3% when compared to the analytical solution. It is important to notice that the predominant frequency is the first one, so the finite element method produces a satisfactory result, when analyzing the unit impulse response of the system. As noticed in Figs. 5 to 10 and 13 to 16, the finite element gives a vibration of higher frequency around the response of the first natural frequency, which is in good agreement with the analytical solution in section 2.5.

Table 2. Comparison of natural frequencies

	14100 rpm				**20280 rpm**			
	ω_{n1} (rad/s)	Percentual difference	ω_{n2} (rad/s)	Percentual difference	ω_{n1} (rad/s)	Percentual difference	ω_{n2} (rad/s)	Percentual difference
Analytical	5264.7	-	151454	-	6528.9	-	151433	-
Lumped parameters	5263.9	0.02%	-	-	6527.3	0.02%	-	-
FE - Mesh 1	5374.0	2.08%	121216	19.97%	6665.7	2.10%	121225	19.95%
FE - Mesh 2	5382.2	2.23%	124458	17.82%	6676.6	2.26%	124467	17.81%
FE - Mesh 3	5417.5	2.90%	121213	19.97%	6729.7	3.08%	121220	19.95%
FE - Mesh 4	5205.7	1.12%	124503	17.79%	6681.0	2.33%	124516	17.77%

4. CONCLUSIONS

The discretization of the shaft and the bearing can be significant to observe the deformation of the shaft and the behavior of the bearing when exciting the system, whether with an impulse or step external force. The theory predicts that the system excited with an impulse tends to the initial equilibrium position after oscillating around it and the system excited with a step changes its equilibrium position and vibrates around the new equilibrium position. It is also possible to notice that the thrust bearing is responsible for the axial damping of the rotating system. In the lumped parameters model (mass-spring-damper system) the response is highly damped, and in the finite element model, the predominant response of the first vibration mode, associated with the lowest natural frequency, is also highly damped. So, the model of the bearing can be considered satisfactory. Hence, the models proposed here to simulate the axial vibration of rotors supported by thrust bearings are promising to represent the dynamic behavior of a rotor-axial bearing system.

5. ACKNOWLEDGEMENTS

The authors thank CNPq, SAE/UNICAMP and BorgWarner for the financial support of this research.

6. REFERENCES

Balachandram, B. & Magrab, E. B., 2009. Vibrations. 2nd ed. Toronto, ON: Cengage Learning.

Bathe, K. J. & Wilson, E. L., 1973. Stability and Accuracy Analysis of Direct Integration Methods. International Journal of Earthquake Engineering and Structural Dynamics, Volume 1, pp. 283-291.

Cook, R. D., Malkus, D. S., Plesha, M. E. & Witt, R. J., 2002. Concepts and Applications of Finite Element Analysis. 4th ed. Hoboken(New Jersey): John Wiley & Sons.

Gupta, K. K., 1974. Eigenproblem Solution of Damped Structural Systems. International Journal for Numerical Methods in Engineering, Volume 8, pp. 877-911.

Müller, P. C. & Schiehlen, W. O., 1985. Linear Vibrations. Dordrecht: Martinus Nijhoff Publishers.

Nelson, H. D., 1980. A finite rotating shaft element using timoshenko beam theory. ASME Journal of Mechanical Design, Volume 102, pp. 793-803.

Nelson, H. D. & McVaugh, J. M., 1976. The Dynamics of Rotor-Bearing Systems Using Finite Elements. ASME Journal of Engineering for Industry, Volume 98, pp. 593-600.

Newmark, N. M., 1959. A Method of Computation for Structural Dynamics. ASCE Journal of Engineering Mechanics Division, Volume 85, pp. 67-94.

Rayleigh, L., 1877. Theory of Sound (two volumes). 2nd ed. New Yotk: Dover Publications.

Vieira, L. C., 2014. Análise de um Modelo Termohidrodinâmico para Mancais Axiais, Campinas, Tese de Doutorado, UNICAMP, Faculdade de Engenharia Mecânica, 242p.

Vieira, L. C. & Cavalca, K. L., 2009. Hydrodynamic Lubrication Evaluation of Sector Thrust Bearings. 20th International Congress of Mechanical Engineering - COBEM 2009, Volume 1, pp. 1-10.

Zhu, Q. & Zhang, W. J., 2003. A Preliminary Nonlinear Analysis of the Axial Transient Response of the Sector-Shaped Hydrodynamic Thrust Bearing-Rotor System. Transactions of the ASME, October, Volume 125, pp. 854-858.

7. RESPONSIBILITY NOTICE

The authors are the only responsible for the printed material included in this paper.